

Old-Growth Forests Can Accumulate Carbon in Soils

Guoyi Zhou,^{1*†} Shuguang Liu,^{2*} Zhian Li,¹ Deqiang Zhang,¹ Xuli Tang,¹ Chuanyan Zhou,¹ Junhua Yan,¹ Jiangming Mo¹

Old-growth forests have traditionally been considered negligible as carbon sinks because carbon uptake has been thought to be balanced by respiration (1). We show that soils in the top 20-cm soil layer in preserved old-growth forests in southern China accumulated atmospheric carbon at an unexpectedly high rate from 1979 to 2003. This phenomenon indicates the need for future research on the complex responses and adaptation of belowground processes to global environmental change.

Understanding the locations and driving forces of carbon sources and sinks at plot-to-global scales is critical for the prediction and management of the global carbon cycle and ultimately the behavior of the Earth's climate system (2). Major uncertainties remain in the geospatial distribution of terrestrial carbon sources and sinks and the mechanisms that drive the distribution and its change. Research efforts have largely been focused on the investigation and quantification of the impacts of climate variability and land use activities on the carbon cycle at various spatial and temporal scales. The soil carbon balance of old-growth forests has received little attention. It is generally accepted that soil organic carbon (SOC) levels in old-growth forests are in a steady state (1). To our knowledge, the long-term dynamics of SOC in old-growth forests and the validity of the above perception have not been tested.

We conducted a study to measure the long-term dynamics (1979 to 2003) of SOC stock in old-growth forests [age > 400 years (3)] at the Dinghushan Biosphere Reserve (23°09'21"N to 23°11'30"N and 112°30'39"E to 112°33'41"E) in Guangdong Province, China. The estimation of SOC stock change requires a series of measurements of SOC concentration, bulk density, and soil thickness taken at different points in time (4, 5). In this study, we observed long-term changes in SOC concentration and bulk density but did not measure changes in soil thickness in the old-growth forests. Although soil thickness dynamics were not monitored, their possible contribution to the uncertainty in the results was analyzed and quantified by using upper and lower bounds of possible SOC change (Materials and Methods).

Results show that SOC concentration in the top 20-cm soil layer increased between 1979 and 2003 from about 1.4% to 2.35% at an average rate of 0.035% each year, which was significantly different from 0 at $\alpha = 0.05$. At the same time, the mean bulk density of the top 20-cm soil layer decreased significantly ($\alpha = 0.05$), with an average rate of 0.0032 g cm⁻³ year⁻¹. Measurements on a total of 230 composite soil samples collected between 1979 and 2003 suggested that SOC stock in the top 20-cm soil layer increased significantly during that time ($P < 0.0001$), with an average rate of 0.61 Mg C ha⁻¹ year⁻¹ (Fig. 1). The lower and upper bounds of this average rate

were 0.54 and 0.68 Mg C ha⁻¹ year⁻¹, after considering the uncertainty introduced by the lack of thickness-change monitoring. We took more than enough samples to detect the observed SOC change. In fact, statistical analysis shows that 20 samples taken every 8 to 10 years of sampling interval (or 100 samples every 5 years) would be sufficient to detect the observed SOC change rate in these forests at a 95% confidence level. More samples would be required at shorter sampling intervals to detect the observed change, given the observed spatial variability of SOC concentration and bulk density.

The driving forces for this observed high rate of SOC increase in the old-growth forests are not clear at present and deserve further study. This study suggests that the carbon cycle processes in the belowground system of these forests are changing in response to the changing environment. This result directly challenges the prevailing belief in ecosystem ecology regarding carbon budget in old-growth forests (1) and supports the establishment of a new, non-equilibrium conceptual framework to study soil carbon dynamics. Our study further highlights the need to focus on the complexity of the belowground processes, as advocated in previous research (6, 7), and the importance of establishing long-term observation studies on the responses of belowground processes to global change.

References and Notes

1. E. P. Odum, *Science* **164**, 262 (1969).
2. Intergovernmental Panel on Climate Change, *Climate Change 2001: The Scientific Basis* (Cambridge Univ. Press, Cambridge, 2001).
3. C. D. Shen *et al.*, *Chin. Sci. Bull.* **44**, 251 (1999).
4. W. M. Post, R. C. Izaurralde, L. K. Mann, N. Bliss, *Clim. Change* **51**, 73 (2001).
5. F. Conen, M. V. Yakutin, A. D. Sambuu, *Glob. Change Biol.* **9**, 1515 (2003).
6. R. Lal, *Science* **304**, 1623 (2004).
7. C. A. Johnston *et al.*, *Front. Ecol. Environ.* **2**, 522 (2004).
8. G.Z. acknowledges support from the Chinese Ecosystem Research Network (CERN), the Chinese Academy of Science (project KSCX2-SW-120), and the Natural Science Foundation of China (project 30470306). S.L.'s work was supported by the USGS Geographic Analysis and Monitoring Program and the Earth Surface Dynamics Program. Work was performed under USGS contract 03CRCN0001.

Supporting Online Material

www.sciencemag.org/cgi/content/full/314/5804/1417/DC1
Materials and Methods
References

18 May 2006; accepted 13 September 2006
10.1126/science.1130168

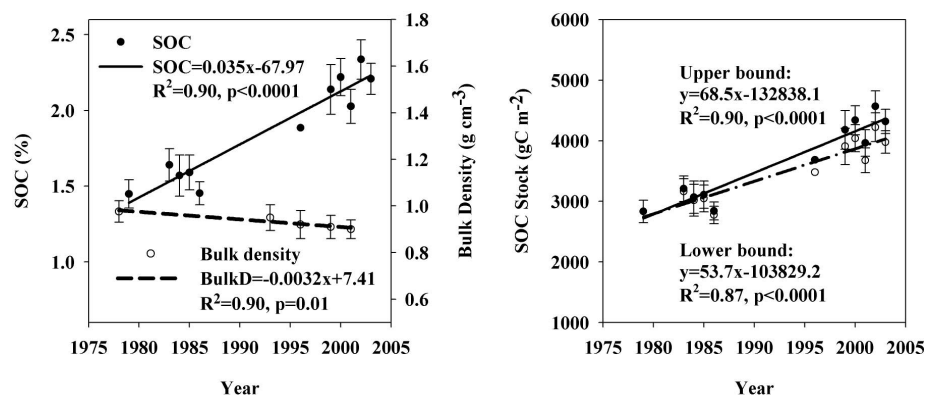


Fig. 1. Temporal changes of (left) soil organic carbon concentration, bulk density, and (right) soil organic carbon stock in the top 20-cm soil layer in broadleaved old-growth forests in Dinghushan Nature Reserve. Upper and lower bounds contain the uncertainty introduced by the lack of monitoring of soil thickness during the study period. Error bars indicate standard deviation.

¹South China Botanical Garden, Chinese Academy of Sciences, Guangzhou, 510650, China. ²SAIC, U.S. Geological Survey (USGS) Center for Earth Resources Observation and Science, Sioux Falls, SD 57198, USA.

*These authors contribute equally to this work.

†To whom correspondence should be addressed. E-mail: gyzhou@scib.ac.cn

Species Interactions Reverse Grassland Responses to Changing Climate

K. B. Suttle,^{1*} Meredith A. Thomsen,² Mary E. Power¹

Predictions of ecological response to climate change are based largely on direct climatic effects on species. We show that, in a California grassland, species interactions strongly influence responses to changing climate, overturning direct climatic effects within 5 years. We manipulated the seasonality and intensity of rainfall over large, replicate plots in accordance with projections of leading climate models and examined responses across several trophic levels. Changes in seasonal water availability had pronounced effects on individual species, but as precipitation regimes were sustained across years, feedbacks and species interactions overrode autecological responses to water and reversed community trajectories. Conditions that sharply increased production and diversity through 2 years caused simplification of the food web and deep reductions in consumer abundance after 5 years. Changes in these natural grassland communities suggest a prominent role for species interactions in ecosystem response to climate change.

Impacts of recent climate change on plants and animals are already evident, as geographic distributions shift poleward (1, 2) and toward higher elevations (3, 4), phenological events advance in time (5–7), and some species disappear altogether (8). With further climate change still expected, prediction of future impacts has become critical to conservation planning and management. To forecast ecological change under continued climate warming, how-

ever, we need a better understanding of the relative importance of direct responses by individual species to climate versus responses mediated by changing interactions with resources, competitors, pathogens, or consumers (9–14). We imposed projected future precipitation regimes over grassland in northern California to evaluate the importance to ecosystem response of direct effects on grassland species versus indirect effects arising from species interactions.

Much of the California coastal region experiences a Mediterranean climate, characterized by wet winters and long summer droughts. Ecological responses to climate change in regions with Mediterranean climate regimes may be strongly driven by the redistribution of water in time and space (15). Changes in seasonal water

availability that affect plant phenology, for example, could lead to temporal mismatch between resource availability and consumer demand (16), which can have important effects on resource flow and ecosystem function (17). General circulation models developed at the Hadley Centre for Climate Prediction and Research (HadCM2) and the Canadian Centre for Climate Modeling and Analysis (CCM1) (18) predict substantial increases in precipitation over most of California but differ in the projected seasonality of these increases. The Hadley model calls for all additional rain to fall during the current winter rainy season, whereas the Canadian model projects increased rainfall extending into the current summer drought. The discrepancy between the two scenarios may be critical to the fate of grassland ecosystems in California, where summer drought severely constrains plant growth and the timing of rainfall is more important to annual production and species composition than the amount (19–22).

In 2001, we began a large-scale rainfall manipulation in a northern California grassland to examine the consequences of these two projected regimes for production and diversity of grassland plants and invertebrates. In a grassland at the Angelo Coast Range Reserve in Mendocino County, California (39° 44' 17.7" N, 123° 37' 48.4" W), 18 circular 70-m² plots were subjected to one of three watering treatments: a winter addition of water (January through March), a spring addition of water (April through June), and an unmanipulated ambient control (Fig. 1). Each watered plot received about 44 cm of supplementary water over ambient rainfall per year, roughly a 20% increase over mean annual precipitation but within natural variability in both amount and timing at the study site (fig. S1). We

¹Department of Integrative Biology, University of California, Berkeley, CA 94720, USA. ²Department of Biology, University of Wisconsin, La Crosse, WI 54601, USA.

*Present address: Earth and Planetary Science, University of California, Berkeley, CA 94720, USA.

†To whom correspondence should be addressed. E-mail: kbsuttle@socrates.berkeley.edu

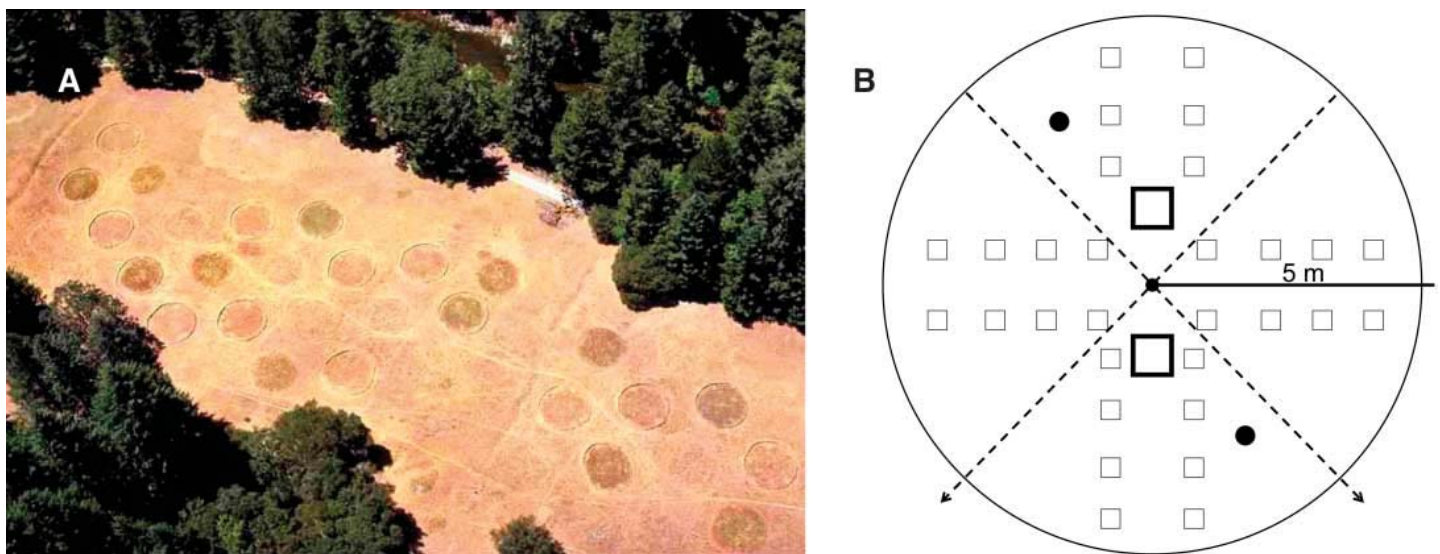


Fig. 1. (A) Bird's-eye view of experimental communities in July 2002. A nearby road is visible as a gray strip, top right. Research described here is from 18 open-grassland plots (18 additional plots were used in separate research). (B) Schematic representation of an experimental plot, shown as partitioned for measurement of plant biomass (30 900-cm²

subplots, small squares), plant species richness (two 2500-cm² subplots, large squares), foliar and flying invertebrates (two perpendicular sweep-net transects, dashed arrows), and ground-dwelling invertebrates (two pitfall traps, circles) (not to scale). Detailed methods are available online (23).

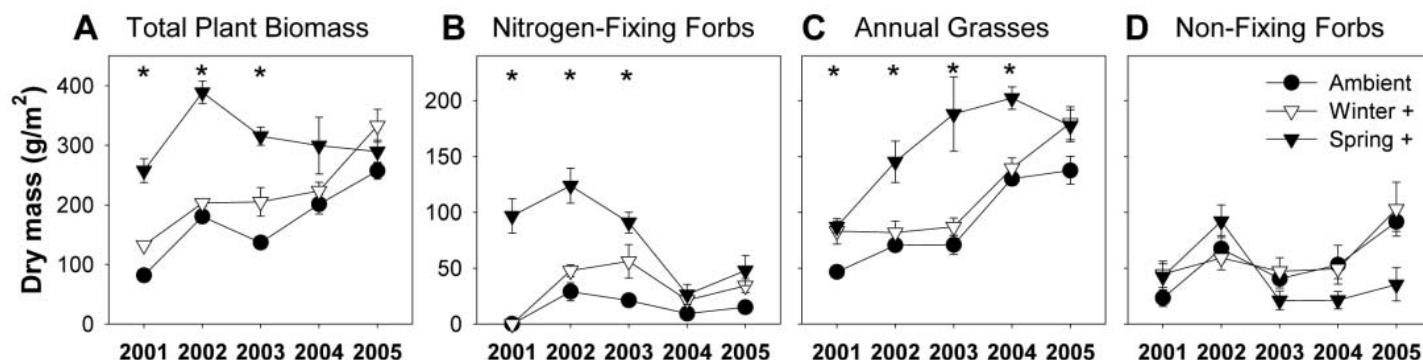


Fig. 2. Watering treatment effects on (A) total plant biomass and (B to D) biomass of individual plant groups (note difference in scales). Data represent treatment means \pm 1 SE. An asterisk denotes a statistically significant treatment difference after Bonferroni correction for multiple comparisons. See Table S1 for factor significance.

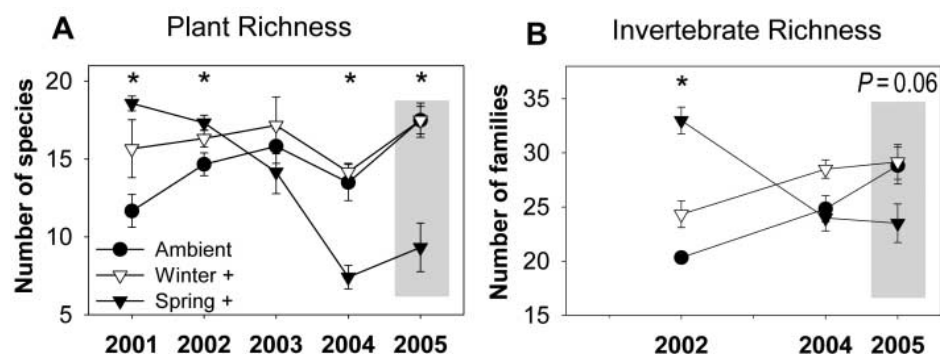


Fig. 3. Watering treatment effects on (A) plant species richness and (B) invertebrate family richness. Data represent treatment means \pm 1 SE. Gray shading highlights the year that late natural rainfall mirrored the spring-addition watering treatment. See tables S2 and S3 for taxonomic listings of plant species and invertebrate families, respectively.

examined treatment effects on plant production and species composition over 5 consecutive years and quantified responses of invertebrate herbivores and their natural enemies over 3 years (23).

Effects of increased rainfall depended critically on the seasonality of the increase. Supplemental water addition during the wet winter period produced moderate increases in plant production in some years of the study (Fig. 2), but effects did not extend to higher trophic levels (Figs. 3 and 4). In general, communities in winter-addition and ambient rainfall plots responded similarly across years to annual variation in rainfall.

Extending the rainy season via spring water addition produced much more dramatic changes in the grassland community. Plant production more than tripled in the first year and more than doubled in the second compared with the control (Fig. 2A). The strongest initial response was by nitrogen-fixing forbs, whose production increased by nearly two orders of magnitude with extended spring rainfall (Fig. 2B). Exotic annual grasses showed a weaker response to the first year of spring water addition, but after the proliferation of nitrogen-fixing forbs that year, annual grass production rose dramatically (Fig. 2C). These grasses, so-called winter annuals because they are the first plants to germinate

each year and are among the earliest to complete their life cycle and senesce, generally do not respond to extensions of the rainy season beyond April (22, 24). Early phenology thus limited the direct response of annual grasses to extended rainfall but allowed these plants to benefit in the subsequent growing season from a fertilization effect after decomposition of abundant N-fixer litter (25–27). As this process was repeated year after year, the accumulation of annual grass litter suppressed germination and regrowth of leafy forbs (Fig. 2D), as has often been seen in California annual grasslands (26, 28–30), and drove steep declines in plant species richness (Fig. 3A).

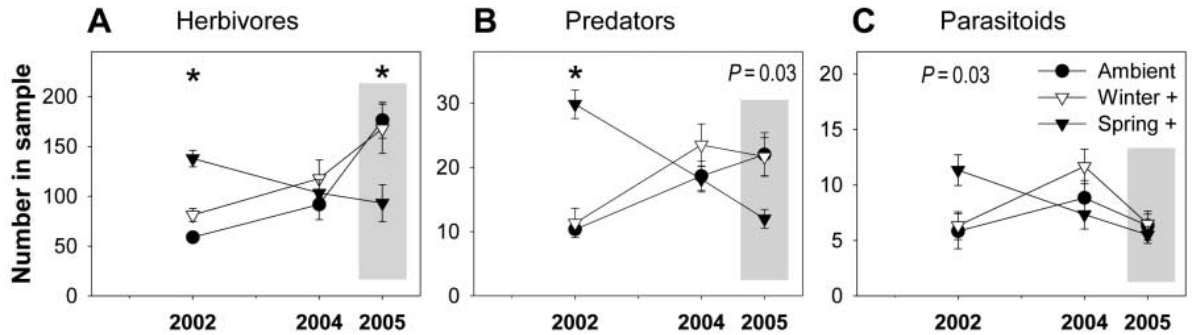
Shifts in plant composition in spring-addition plots had important consequences for biodiversity and food web structure. Initially, extended rainfall promoted increased plant species richness (Fig. 3A), and this increase, coupled with greater primary production and water availability, supported greater diversity and abundance of invertebrate herbivores, predators, and parasitoids (Figs. 3B and 4). As forbs were eliminated from spring-addition plots by annual grasses, however, plant species richness collapsed to nearly half that in control plots. With early-senescing annual grasses increasingly dominating the resource base, food availability and habitat quality for higher trophic levels dimin-

ished. This was especially true during summer, when late-blooming forbs provide a critical food resource for invertebrate herbivores (fig. S2). In contrast, annual grass litter has low nutritional value, and monocultures of these plants offer less structural complexity than mixed grass-forb assemblages.

By the fifth year of the study, when heavy rains continued into summer in a naturally extended rainy season throughout northern California, spring-addition plots stood out as islands of low biodiversity and reduced consumer abundances (Fig. 3B and 4). In addition to the nearly 50% reduction in plant species richness in spring-addition relative to control plots, invertebrate richness was 20% lower, and herbivore and predator abundances were each nearly 50% lower than ambient values measured in control plots. This simplification of the grassland community did not result from climatic conditions that were inherently unfavorable to production and diversity. Species at every trophic level benefited strongly from experimental extension of the rainy season in spring-addition plots early in the study, just as they did from a natural extension of the rainy season in winter-addition and control plots late in the study. But as altered environmental conditions persisted across years, individualistic responses by species to climate were overshadowed by the lagged effects of altered community-level interactions. The congruence between initial responses to artificial extension in spring-addition plots and responses in the grassland as a whole to naturally late rainfall in year 5 provides compelling evidence that these mechanisms are real rather than experimental artifacts.

Uncertainty remains in the projections of global climate models; indeed, the next-generation Hadley model (HadCM3) forecasts decreased rainfall over much of California (31). Yet under any scenario of future climate change, prediction of ecological effects will require understanding the web of interactions that mediate species- through ecosystem-level responses (14). To date, forecasts of range shifts and extinction probabilities are based largely on species-climate envelope models (32–34). These models are powerful initial tools

Fig. 4. Watering treatment effects on abundances (mean \pm SE) of (A) invertebrate herbivores, (B) predators, and (C) parasitoids, as measured in sweep net and pitfall trap collections. Gray shading highlights responses in the final year of the study, when late natural rainfall mirrored the spring-addition watering treatment.



with which to explore consequences of alternative climate scenarios, but they cannot forecast lagged impacts of altered higher-order interactions that will govern the trajectories of ecosystems under sustained climatic change. Nonlinearities are expected from the assembly of new combinations of species brought together by climate-induced range shifts, but these can also arise from environmental effects on the strength and direction of interspecific interactions without any change in species composition (35, 36). The nature and scales of these effects are best revealed by long-term experiments in natural field settings that improve understanding of how climate change impacts propagate through ecological communities. Indirect effects of climate on species will commonly lag behind direct effects, but their importance makes system-level interactions crucial to climate change forecasting even at subdecadal time scales.

(Union of Concerned Scientists and Ecological Society of America, Cambridge, MA, 1999).

- M. D. Pitt, H. F. Heady, *Ecology* **59**, 336 (1978).
- Information on materials and methods is available on Science Online.
- L. E. Jackson, J. Roy, *Acta Oecol.* **7**, 191 (1986).
- J. R. Bentley, L. R. Green, *J. Range Manage.* **7**, 25 (1954).
- J. R. Bentley, L. R. Green, K. A. Wagnon, *J. Range Manage.* **11**, 133 (1958).
- M. B. Jones *et al.*, *J. Prod. Agric.* **3**, 534 (1990).
- H. F. Heady, *Ecology* **39**, 402 (1958).
- R. J. Hobbs, S. L. Gulmon, V. J. Hobbs, H. A. Mooney, *Oecologia* **75**, 291 (1988).
- L. F. Huenneke, S. P. Hamburg, R. Koide, H. A. Mooney, P. M. Vitousek, *Ecology* **71**, 478 (1990).
- V. D. Pope, M. L. Gallani, P. R. Rowntree, R. A. Stratton, *Clim. Dyn.* **16**, 123 (2000).
- A. T. Peterson *et al.*, *Nature* **416**, 626 (2002).
- C. D. Thomas *et al.*, *Nature* **427**, 145 (2004).
- W. Thuiller, S. Lavorel, M. B. Araujo, M. T. Sykes, J. C. Prentice, *Proc. Natl. Acad. Sci. U.S.A.* **102**, 8245 (2005).
- K. D. Rothley, G. Dutton, *Can. J. Zool.* **84**, 1053 (2006).

- J. R. Lensing, D. H. Wise, *Proc. Natl. Acad. Sci. U.S.A.* **103**, 15502 (2006).
- We thank J. Bastow, C. McNeely, J. Miner, T. Popp, and J. Sapp for assistance in the field; J. Banfield and the Banfield lab group for constructive discussions of these ideas; J. Abraham, W. Palen, A. Sugden, and three anonymous referees for critical readings of the manuscript; C. Barr, B. Zuparko, and the Essig Museum of Entomology at UC Berkeley for assistance with invertebrate taxonomy; and P. Steel and the University of California Natural Reserve System for protection and stewardship of the study site. This work was supported by an Environmental Protection Agency Science to Achieve Results Fellowship and a Canon National Parks Science Scholarship to K.B.S.

Supporting Online Material

www.sciencemag.org/cgi/content/full/315/5812/640/DC1
 Materials and Methods
 Figs. S1 and S2
 Tables S1 to S3
 17 October 2006; accepted 13 December 2006
 10.1126/science.1136401

References and Notes

- C. Parmesan *et al.*, *Nature* **399**, 579 (1999).
- C. D. Thomas, J. J. Lennon, *Nature* **399**, 213 (1999).
- G. Grabherr, M. Gottfried, H. Paull, *Nature* **369**, 448 (1994).
- M. Sanz-Elorza, E. D. Dana, A. Gonzalez, E. Sobrino, *Ann. Bot. (London)* **92**, 273 (2003).
- T. J. C. Beebee, *Nature* **374**, 219 (1995).
- H. Q. P. Crick, C. Dudley, D. E. Glue, D. L. Thomson, *Nature* **388**, 526 (1997).
- A. H. Fitter, R. S. R. Fitter, *Science* **296**, 1689 (2002).
- J. A. Pounds, M. P. L. Fogden, J. H. Campbell, *Nature* **398**, 611 (1999).
- A. R. Ives, *Ecology* **76**, 926 (1995).
- A. J. Davis, L. S. Jenkinson, J. H. Lawton, B. Shorrocks, S. Wood, *Nature* **391**, 783 (1998).
- E. Post, R. O. Peterson, N. C. Stenseth, B. E. McLaten, *Nature* **401**, 905 (1999).
- G. R. Walther *et al.*, *Nature* **416**, 389 (2002).
- C. E. Burns, K. M. Johnston, O. J. Schmitz, *Proc. Natl. Acad. Sci. U.S.A.* **100**, 11474 (2003).
- O. J. Schmitz, E. Post, C. E. Burns, K. M. Johnston, *Bioscience* **53**, 1199 (2003).
- A. Gasith, V. H. Resh, *Annu. Rev. Ecol. Syst.* **30**, 51 (1999).
- W. Voigt *et al.*, *Ecology* **84**, 2444 (2003).
- M. Winder, D. E. Schindler, *Ecology* **85**, 2100 (2004).
- National Assessment Synthesis Team, *Climate Change Impacts on the United States: The Potential Consequences of Climate Variability and Change* (U.S. Global Change Research Program, Washington, DC, 2000).
- J. Bartolome, *J. Ecol.* **67**, 273 (1979).
- N. L. Stephenson, *Am. Nat.* **135**, 649 (1990).
- C. B. Field *et al.*, *Confronting Global Climate Change in California: Ecological Impacts on the Golden State*

An X Chromosome Gene, *WTX*, Is Commonly Inactivated in Wilms Tumor

Miguel N. Rivera,^{1,2,3} Woo Jae Kim,¹ Julie Wells,¹ David R. Driscoll,¹ Brian W. Brannigan,¹ Moonjoo Han,² James C. Kim,² Andrew P. Feinberg,⁴ William L. Gerald,⁵ Sara O. Vargas,⁶ Lynda Chin,⁷ A. John Iafrate,² Daphne W. Bell,^{1*} Daniel A. Haber^{1†}

Wilms tumor is a pediatric kidney cancer associated with inactivation of the *WT1* tumor-suppressor gene in 5 to 10% of cases. Using a high-resolution screen for DNA copy-number alterations in Wilms tumor, we identified somatic deletions targeting a previously uncharacterized gene on the X chromosome. This gene, which we call *WTX*, is inactivated in approximately one-third of Wilms tumors (15 of 51 tumors). Tumors with mutations in *WTX* lack *WT1* mutations, and both genes share a restricted temporal and spatial expression pattern in normal renal precursors. In contrast to biallelic inactivation of autosomal tumor-suppressor genes, *WTX* is inactivated by a monoallelic "single-hit" event targeting the single X chromosome in tumors from males and the active X chromosome in tumors from females.

Wilms tumor (nephroblastoma) is the most common pediatric kidney cancer and is derived from pluripotent renal precursors that produce undifferentiated blastemal cells, primitive epithelial structures, and stro-

mal components [reviewed in (1)]. In 1972, Knudson and Strong proposed that Wilms tumor, like retinoblastoma, may develop as a consequence of two independent rate-limiting genetic events, subsequently defined as biallelic

feature was visible near the expected locations. The 3- σ upper limit to the disk-integrated I/F of any undetected satellite, derived from individual 120-s exposures, is 30 km² (3). For comparison, Mab had a disk-integrated I/F of 50 km² in the HST data, while near maximum elongation as in our October images. This moon is thus very dark near 2 μ m, suggestive of absorption by water ice. This makes Mab comparable in surface composition to the five "classical" moons Miranda through Oberon, whose spectra show deep (factor 2 to 3) water ice absorption features near 2 μ m. In contrast, Uranus's small inner moons are neutral to slightly red throughout the visual-infrared (6, 7), suggesting that water ice is absent from their surfaces. Mab orbits midway between these two populations. Because of its tiny size, Showalter and Lissauer (1) assumed that Mab would resemble the inner moons, with a small geometric albedo (7 to 10%). Our data suggest that Mab may be covered by ice and therefore be as bright as the outer moons (albedo 20 to 40%). This would decrease Mab's estimated radius from 12 km to 6 to 8 km and hence means that Mab, rather than Cupid (~8 km), is Uranus' smallest regular satellite.

In 2007, Uranus' ring system will appear edge-on to Earth, making faint rings ~100 times brighter and enabling measurements of their vertical extent. If indeed similar physical processes are at work within R1 as in Saturn's E ring, then particles in R1 must also be subject to vertical perturbations, resulting in a vertically extended ring. This can be verified in 2007.

References and Notes

1. M. R. Showalter, J. J. Lissauer, *Science* **311**, 973 (2006).
2. I. de Pater, S. G. Gibbard, H. B. Hammel, *Icarus* **180**, 186 (2006).
3. Materials and methods are available as supporting material on *Science* Online.
4. J. A. Burns, D. P. Hamilton, M. R. Showalter, in *Interplanetary Dust*, E. Grün, B. A. S. Gustafson, S. F. Dermott, H. Fechtig, Eds. (Springer-Verlag, Berlin), pp. 641–725 (2001).
5. R. G. French, P. D. Nicholson, C. C. Porco, E. A. Marouf, in *Uranus*, J. T. Bergstrahl, E. D. Miner, M. S. Matthews, Eds. (Univ. Arizona Press, Tucson), pp. 327–409 (1991).
6. E. Karkoschka, *Icarus* **151**, 51 (2001).
7. S. G. Gibbard, I. de Pater, H. B. Hammel, *Icarus* **174**, 253 (2005).
8. M. R. Showalter, J. N. Cuzzi, S. M. Larson, *Icarus* **94**, 451 (1991).
9. I. de Pater, S. C. Martin, M. R. Showalter, *Icarus* **172**, 446 (2004).
10. M. M. Hedman *et al.*, *BAAS* **37** #66.02 (2005).
11. M. R. Showalter, J. N. Cuzzi, *Icarus* **103**, 124 (1993).

12. H. B. Throop, L. W. Esposito, *Icarus* **131**, 152 (1998).
13. J. A. van Allen, M. F. Thomson, B. A. Randall, R. L. Rairden, C. L. Grosskreutz, *Science* **207**, 415 (1980).
14. T. Johnson, American Geophysical Union, Fall Meeting, San Francisco, 5–9 December 2005, P21F-03.
15. M. Horányi, J. A. Burns, D. P. Hamilton, *Icarus* **97**, 248 (1992).
16. A. Juhász, M. Horányi, *J. Geophys. Res.* **107**, 1 (2002).
17. This work was funded by the National Science Foundation and Technology Center for Adaptive Optics, managed by the University of California at Santa Cruz under cooperative agreement AST-9876783. The W. M. Keck Observatory is operated as a scientific partnership among the California Institute of Technology, the University of California, and the National Aeronautics and Space Administration and was built with financial support of the W. M. Keck Foundation. Further support was provided by NASA grants NAG5-11961 and NAG5-10451 (H.B.H.), NNG05GL48G (M.R.S.), and proposal numbers GO-9823, 10102, and 10274 from the Space Telescope Science Institute, operated by the Association of Universities for Research in Astronomy, under NASA contract NAS5-26555. S.G.'s work was performed under the auspices of the U.S. Department of Energy, National Nuclear Security Administration, by the University of California, Lawrence Livermore National Laboratory under contract W-7405-Eng-48.

Supporting Online Material

www.sciencemag.org/cgi/content/full/312/5770/92/DC1
Materials and Methods
References

18 January 2006; accepted 2 March 2006
10.1126/science.1125110

Deconvolution of the Factors Contributing to the Increase in Global Hurricane Intensity

C. D. Hoyos,* P. A. Agudelo, P. J. Webster, J. A. Curry

To better understand the change in global hurricane intensity since 1970, we examined the joint distribution of hurricane intensity with variables identified in the literature as contributing to the intensification of hurricanes. We used a methodology based on information theory, isolating the trend from the shorter-term natural modes of variability. The results show that the trend of increasing numbers of category 4 and 5 hurricanes for the period 1970–2004 is directly linked to the trend in sea-surface temperature; other aspects of the tropical environment, although they influence shorter-term variations in hurricane intensity, do not contribute substantially to the observed global trend.

Recent publications linking an increase in hurricane intensity to increasing tropical sea-surface temperatures (SSTs) (1–5) have fueled the debate on whether global warming is causing an increase in hurricane intensity (6, 7). The arguments associating the increase in hurricane intensity with increasing SSTs (1) note positive trends in both global tropical SST and the number of category 4 and 5 hurricanes (NCAT45). The physical mechanism linking the increases in tropical SST and NCAT45 is the theory of maximum potential intensity (3).

The analysis presented in (1) established the existence of coincident positive trends of tropical SST and NCAT45 in each of the ocean basins. Outstanding issues in understanding the substantial increase in global NCAT45 since 1970 include (i) identification of the contributions of natural internal variability on decadal and shorter time scales as compared to a longer-term trend and (ii) identification of the importance of SST in causing the increase in NCAT45, relative to other known variables that influence hurricane intensity (8, 9).

To address these issues, we analyzed the time series of SST, specific humidity in the layer extending from 925 to 500 millibars (mb), wind shear between 850 and 200 mb, and the 850-mb zonal stretching deformation (the change of

zonal wind with longitude). Increasing SST, increasing specific humidity, minimal vertical wind shear, and negative stretching deformation are associated with increasing hurricane intensity. The data sets used in this analysis were the hurricane data set described in (1), the National Oceanic and Atmospheric Administration Extended Reconstructed SST data set (10), and the National Centers for Environmental Prediction/National Center for Atmospheric Research Reanalysis (11). The analysis was conducted for seasonally averaged values for the period 1970–2004 for global hurricanes, including data from the North Atlantic (NATL), West Pacific (WPAC), East Pacific (EPAC), South Pacific (SPAC), South Indian (SIO), and North Indian (NIO) Oceans. Hence, the data set consisted of data points for 35 seasons and six different ocean basins, for a total sample size of 210.

Figure 1 shows a clear positive trend in SST in each of the ocean basins. Although there is no consistent global trend of specific humidity, wind shear, and stretching deformation, there are statistically significant trends [as per the Mann-Kendall approach (12)] in several of the basins (Table 1): in the EPAC, a positive trend in specific humidity; in the SPAC, a negative trend in stretching deformation at 850 mb; and in the NATL, a negative trend in wind shear. It is important to note that these particular trends reinforce the necessary conditions for hurricane formation. The SST trends are not only statistically significant in each of the ocean basins but also have the largest magnitude, except for the SPAC, where stretching defor-

School of Earth and Atmospheric Sciences, Georgia Institute of Technology, Atlanta, GA 30332, USA.

*To whom correspondence should be addressed. E-mail: choyos@eas.gatech.edu

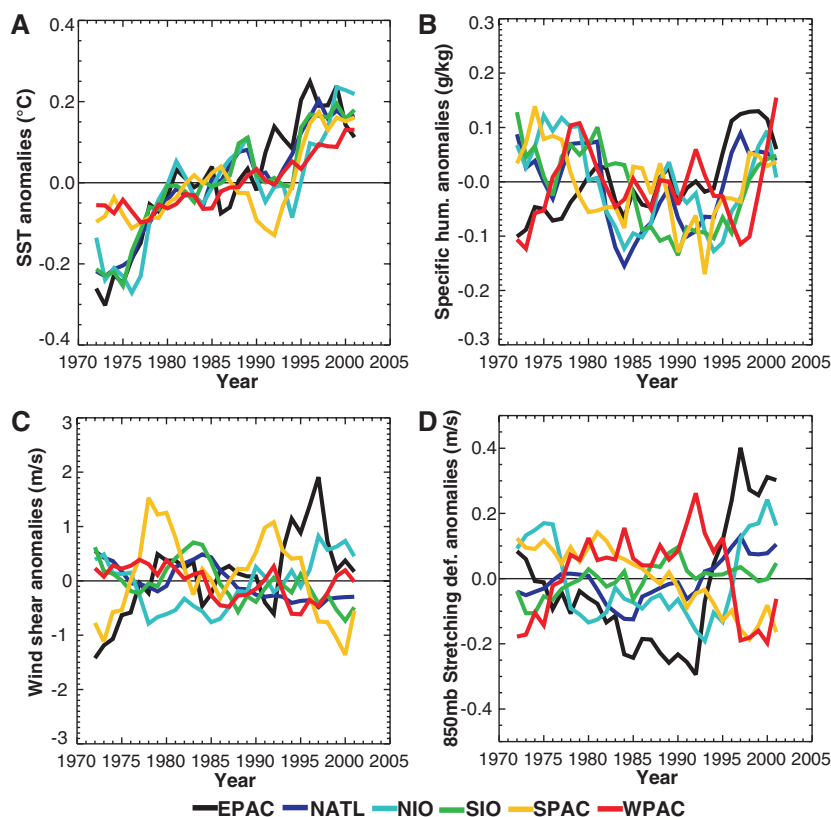


Fig. 1. Five-year moving average anomalies relative to the 1970–2004 period for the EPAC (90° to 120°W, 5° to 20°N, June–October), NATL (90°W to 20°E, 5° to 25°N, June–October), NIO (55° to 90°E, 5° to 20°N, April–May and September–November), SIO (50° to 115°E, 5° to 20°S, November–April), SPAC (155° to 180°E, 5° to 20°S, December–April), and WPAC (120° to 180°E, 5° to 20°N, May–December). Basins and seasons are defined by (1) for (A) SST, (B) specific humidity, (C) wind shear, and (D) stretching deformation at 850 mb.

Table 1. Standardized trends (per 35 years) for all variables in each basin for the period 1970–2004.

Basin	SST	Specific humidity	Wind shear	Stretching deformation (850 mb)
EPAC	1.934*	1.228*	0.827	0.581
NATL	2.767*	0.058	−1.880*	1.208
NIO	2.017*	−0.971	0.315	−0.134
SIO	2.095*	−0.653	−1.468	0.734
SPAC	1.788*	−0.159	−0.035	−1.840*
WPAC	2.046*	0.803	−0.562	0.376

*Values are significantly different than zero at the 99% confidence level.

mation at 850 mb also presents a trend of comparable magnitude.

To understand the relationships between NCAT45 and the four variables considered, we used a methodology based on information theory, whereby the mutual information (MI) of both variables is quantified to represent the measure of independence of the two variables (13). Specifically, the MI quantifies the distance between the joint distribution of two variables, *X* and *Y*, and the product of their marginal distributions. MI can be thought of as a measure of the information of *X* that is shared by *Y*. If *X* and *Y* are independent, then *X* contains no information about *Y* and vice versa, so their MI is zero [see supporting online material (14)].

To quantify the MI, it is necessary to estimate the marginal distribution of the variables. Figure 2, A and B, shows the distributions of NCAT45 and SST. If these two variables were statistically independent, the product of their marginal distributions should replicate their joint distribution (Fig. 2C). The fact that this is not seen for NCAT45 and SST implies that there is statistical dependence between the variables. The joint distribution (Fig. 2D) indicates that statistically, the average SST during each basin’s hurricane season should be high in order to have a larger value of NCAT45. That is, high SST is important not only during the lifetime of a single event (15, 16), but the average SST conditions of the basin seem to be

highly linked with the probability of occurrence of NCAT45. The scaled distribution [the joint distribution scaled by the marginal distribution (Fig. 2E)] shows that higher values associated with their MI [0.51 bits (17)] are located along the diagonal and mainly in its upper part, confirming that the seasonal values of SST are intimately related to NCAT45.

To address the issue of the relative importance of the MI between NCAT45 and SST versus the other variables, we performed the same MI statistical analysis. For specific humidity (Fig. 3A), the analysis indicates that the MI is 0.49 bits. Higher seasonal average values of specific humidity are associated with higher values of NCAT45, with no high NCAT45 associated with low values of specific humidity. Wind shear (Fig. 3B) also shows a relationship with NCAT45 (0.44 bits), with values associated with high values of NCAT45 in the bottom half of the distribution. In other words, high NCAT45 is more likely to occur when the wind shear tends to be low relative to its distribution. In the case of stretching deformation (Fig. 3C), it is clear that the occurrence of high NCAT45 always corresponds to negative values of stretching deformation (9) and explains most of the MI, which is 0.68 bits.

The values of the MI presented in Figs. 2 and 3 are roughly comparable in magnitude, ranging from a high value of 0.68 bits for stretching deformation to a low value of 0.44 bits for wind shear. Because this analysis does not directly allow for distinguishing whether these relationships arise from the long-term trend or the shorter-term modes of natural internal variability (on a decadal scale or shorter), we performed the MI analysis on the isolated trend/variability time series (14). The trend is removed by subtracting the least-squares linear fit from each basin’s variable time series. This method has a physical interpretation only if the trend has a consistent sign in all of the ocean basins and is statistically significant. Hence, this particular analysis is applied only to SST.

Figure 4 shows the results for SST trend time series (Fig. 4A) and SST variability time series (Fig. 4B). The MI is higher when the trend (0.54 bits), in contrast to the variability (0.30 bits), is isolated, and the trend value is comparable to that of the original signal (0.51 bits). In addition, it can be observed that the scaled distribution of the trend is very similar to that of the original variable (Fig. 4A versus Fig. 2E). The high values of NCAT45 appear to be associated with high SST (the upper part of the diagonal) when the trend is isolated (Fig. 4A); however, this is not the case for the variability, which is very symmetrical around the median (Fig. 4B). This implies statistically that the trend in SST accounts for the information associated with the occurrence of high values of NCAT45, whereas the shorter-term variability in SST does not account for a

large proportion of the variance of the high NCAT45.

Recently, the quality of the hurricane data has been questioned (4, 5), and a reanalysis of the tropical cyclone databases has even been suggested in order to confirm that the results of recent studies (1, 2) are not due to problems in the data. Because the NIO hurricane data set has been directly questioned because of potential problems, especially during the 1970s, we performed the MI analysis excluding this basin, obtaining similar results pointing to the same conclusions reached when all six basins were used (fig. S4). In addition, we analyzed the behavior of the seasonal tropospheric moist static stability for all six basins. We found a statistically significant and strong negative trend in this variable for five of the six basins (fig. S5), indicating a more unstable troposphere. Interestingly, although the EPAC shows no trend in the moist static stability index, it is the only basin that presents a significant positive trend in the specific humidity (Table 1). These results support the physical connection between ocean and atmosphere for the link between increasing SST and NCAT45.

An outstanding issue is to investigate whether the SST variation is the primary source of information shared with the NCAT45 trend in the three basins that possessed statistically significant trends in other variables: the EPAC specific humidity, the SPAC stretching deformation at 850 mb, and the NATL vertical wind shear. Because the number of data points for each basin is only 35, we could not apply the MI technique. Hence, we conducted a correlation analysis on the complete and detrended time series for each of these basins (Table 2). The correlation between humidity and NCAT45 in the EPAC is not statistically significant. The correlation between stretching deformation and NCAT45 in the SPAC is statistically significant, but the correlation arises almost entirely from the short-term internal variability. The correlation between wind shear and NCAT45 in the NATL is statistically significant, but the correlation is dominated by the short-term variability.

Unfortunately, the sample size for the individual basins is too small to reliably test the significance of the difference between the correlation for the original time series and that for the detrended time series. The same correlation analysis shown in Table 2 for SST (18) reveals that the correlation for SST in the original time series is more than twice as large as for the detrended time series. This analysis suggests that the only basins where there may be some significant contribution of trend from variables besides SST are the NATL and the SPAC. Although this analysis cannot determine quantitatively the relative contributions of SST versus vertical wind shear to the NCAT45 trend in the NATL and versus zonal stretching deformation in the SPAC, the relative differences in the

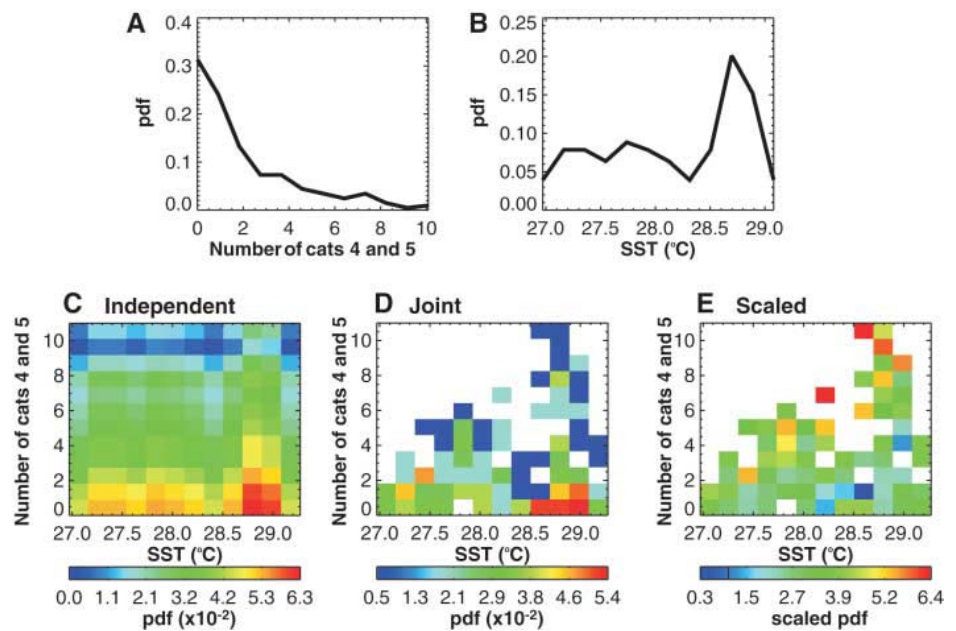


Fig. 2. Marginal distributions in all basins for (A) NCAT45 and (B) SST. pdf, probability density function. (C) Product of the marginal distributions, (D) joint distribution, and (E) scaled distribution for (A) and (B).

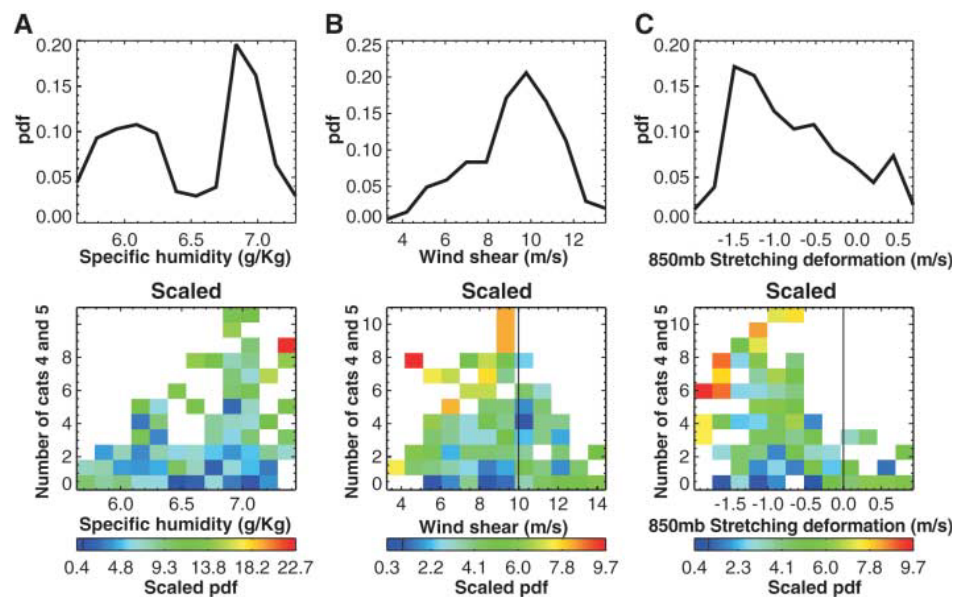


Fig. 3. (A to C) Marginal and scaled distribution for (B) to (D) in Fig. 1. The vertical black line in the bottom panels of (B) and (C) corresponds to the median of the distribution in (B) and to zero in (C).

magnitudes of correlations for the complete versus the detrended time series indicate that the contribution from SST dominates in both basins in contributing to the trend in NCAT45.

Our results show that seasonally averaged values of tropical SST, tropospheric humidity, vertical wind shear, and zonal stretching deformation share information content with the total number of NCAT45 in a season. The shared information content with tropospheric humidity, vertical wind shear, and zonal stretching deformation is dominated by short-term variability, whereas the shared information content with SST is dominated by the longer-term trend. The

implication of these results is that the strong increasing trend in NCAT45 for the period 1970–2004 is directly linked to the trend in tropical SST, and that other aspects of the tropical environment, although they influence shorter-term variations in hurricane intensity, do not contribute significantly to the global trend of increasing hurricane intensity. We infer that there is some contribution to the long-term trend from wind shear in the NATL and from stretching deformation in the SPAC, but that the contribution from SST remains dominant in these basins in contributing to the trend in NCAT45.

Fig. 4. Marginal and scaled distribution for (A) the SST trend time series and (B) the detrended SST variability time series. Values greater than one (the vertical line in the color bar at the bottom) account for the MI shared between the variables.

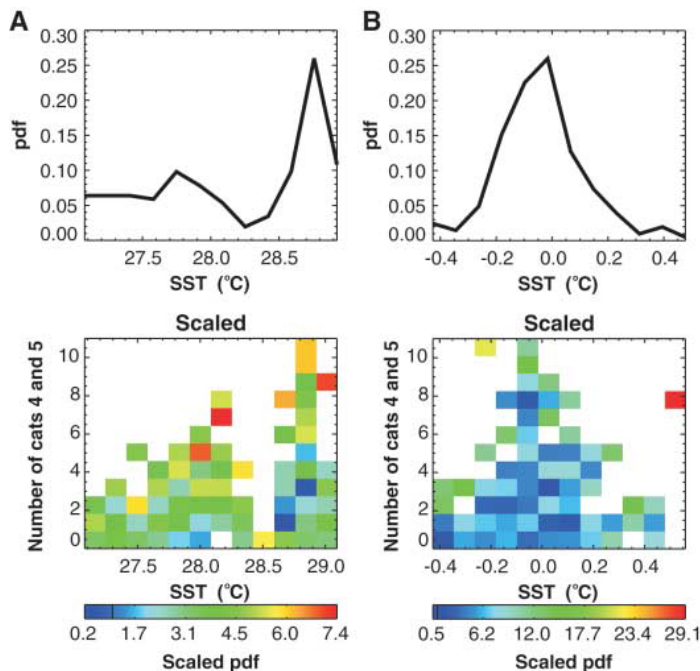


Table 2. Correlations for individual ocean basins between NCAT45 and variables for which there is a statistically significant trend in that basin, for the original time series in bold and the detrended time series in parentheses. NA, not applicable.

Variable	EPAC	NATL	SPAC
SST	0.32* (0.06)	0.67* (0.20)	0.29 (-0.10)
Specific humidity	0.23 (0.13)	NA	NA
Wind shear	NA	-0.61* (-0.45)*	NA
Stretching deformation	NA	NA	-0.67* (-0.55)*

*Statistically significant correlations at the 95% confidence level.

References and Notes

1. P. J. Webster, G. J. Holland, J. A. Curry, H.-R. Chang, *Science* **309**, 1844 (2005).
2. K. E. Trenberth, *Science* **308**, 1753 (2005).
3. K. Emanuel, *Nature* **436**, 686 (2005).
4. C. W. Landsea, *Nature* **438**, E11 (2005).
5. K. Emanuel, *Nature* **438**, E13 (2005).
6. J. A. Curry, P. J. Webster, G. J. Holland, in preparation.
7. R. A. Pielke Jr., C. Landsea, M. Mayfield, J. Laver, R. Pasch, *Bull. Am. Meteorol. Soc.* **86**, 1571 (2005).
8. L. J. Shapiro, S. B. Goldenberg, *J. Clim.* **11**, 578 (1998).
9. P. J. Webster, G. J. Holland, R. A. Houze Jr., paper presented at the 85th American Meteorological Society Annual Meeting, the Ed Lorenz Symposium, San Diego, CA, 13 January 2005 (http://ams.confex.com/ams/Annual2005/techprogram/paper_87148.htm).
10. T. M. Smith, R. W. Reynolds, *J. Clim.* **17**, 2466 (2004).
11. E. M. Kalnay et al., *Bull. Am. Meteorol. Soc.* **77**, 437 (1996).
12. R. M. Hirsch, J. R. Slack, R. Smith, *Water Resour. Res.* **18**, 107 (1982).
13. C. E. Shannon, *Bell System Tech. J.* **27**, 379 (1948).
14. Information on the statistical method is available as supporting material on Science Online.
15. J. Lighthill et al., *Bull. Am. Meteorol. Soc.* **75**, 2147 (1994).
16. W. M. Gray, *Mon. Weather Rev.* **96**, 669 (1968).
17. Values of MI vary from 0 (total independence) to 2.8 (total dependence), corresponding to the entropy of NCAT45 (minimum among all variables).
18. SST correlations for the remaining three basins are as follows (using the same notation as in Table 2): WPAC **0.44*** (0.13), NIO **0.28** (-0.10), SIO **0.54*** (0.02).
19. This research was supported by the Climate Dynamics Division of NSF under award NSF-ATM 0328842.

Supporting Online Material

www.sciencemag.org/cgi/content/full/1123560/DC1
SOM Text
Figs. S1 to S5
Reference

7 December 2005; accepted 7 March 2006
Published online 16 March 2006;
10.1126/science.1123560

Include this information when citing this paper.

Evolution of Hormone-Receptor Complexity by Molecular Exploitation

Jamie T. Bridgham, Sean M. Carroll, Joseph W. Thornton*

According to Darwinian theory, complexity evolves by a stepwise process of elaboration and optimization under natural selection. Biological systems composed of tightly integrated parts seem to challenge this view, because it is not obvious how any element's function can be selected for unless the partners with which it interacts are already present. Here we demonstrate how an integrated molecular system—the specific functional interaction between the steroid hormone aldosterone and its partner the mineralocorticoid receptor—evolved by a stepwise Darwinian process. Using ancestral gene resurrection, we show that, long before the hormone evolved, the receptor's affinity for aldosterone was present as a structural by-product of its partnership with chemically similar, more ancient ligands. Introducing two amino acid changes into the ancestral sequence recapitulates the evolution of present-day receptor specificity. Our results indicate that tight interactions can evolve by molecular exploitation—recruitment of an older molecule, previously constrained for a different role, into a new functional complex.

The ability of mutation, selection, and drift to generate elaborate, well-adapted phenotypes has been demonstrated theoretically (1, 2), by computer simulation (3, 4), in the laboratory (5, 6), and in the field (7). How evolutionary processes assemble complex systems that depend on specific interactions among

the parts is less clear, however. Simultaneous emergence of more than one element by mutational processes is unlikely, so it is not apparent how selection can drive the evolution of any part or the system as a whole. Most molecular processes are regulated by specific interactions, so the lack of exemplars for the emergence of

such systems represents an important gap in evolutionary knowledge. As Darwin stated, "If it could be demonstrated that any complex organ existed which could not possibly have been formed by numerous, successive, slight modifications, my theory would absolutely break down" (8).

The functional interaction between the steroid hormone aldosterone and its specific partner the mineralocorticoid receptor (MR)—a ligand-activated transcriptional regulator (9, 10)—illustrates this evolutionary puzzle. MR and the glucocorticoid receptor (GR) descend from a gene duplication deep in the vertebrate lineage (11) and now have distinct signaling functions. In most vertebrates, GR is specifically activated by the stress hormone cortisol to regulate metabolism, inflammation, and immunity (9). MR is activated by aldosterone to control electrolyte homeostasis and other processes (9, 12). MR can also be activated by cortisol, although the presence of a cortisol-

Center for Ecology and Evolutionary Biology, University of Oregon, Eugene, OR 97403, USA.

*To whom correspondence should be addressed. E-mail: joet@uoregon.edu